Vacancy charging on Si(100)-(2×1): Consequences for surface diffusion and STM imaging

Ho Yeung H. Chan, Kapil Dev, and E. G. Seebauer*
Department of Chemical Engineering, University of Illinois, Urbana, Illinois 61801
(Received 4 February 2002; revised manuscript received 14 May 2002; published 16 January 2003)

The present work investigates the structure and energetics of charged vacancies on Si(100)-(2×1) by calculations using density functional theory. The calculations predict multiple stable charge states for all vacancy structures investigated, although the neutral state is most stable for typical Si(100) surfaces. The multiplicity of possible states lends significant support to a hypothesized mechanism for nonthermal illumination influences on surface diffusion. The calculations also show that the +1 state of the upper dimer monovacancy is destabilized by structural relaxations, leading to negative-*U* properties. Implications of this work for possible artifacts in imaging by scanning tunneling microscopy are discussed.

DOI: 10.1103/PhysRevB.67.035311 PACS number(s): 68.35.Dv, 68.35.Fx, 68.37.Ef, 72.20.−i

I. INTRODUCTION

It has long been known that bulk defects in semiconductors exert powerful effects on the electronic properties of these materials and consequently on the performance of devices fabricated from them. As microelectronic device dimensions continue to scale downward and surface-to-volume ratios increase, there is increasing recognition that analogous defects on semiconductor surfaces exert correspondingly powerful effects.

Studies by this laboratory over the past decade have shown[1] that terrace vacancy defects play an important role in mediating surface mass transport during high-temperature processing steps such as epitaxial film deposition, diffusional smoothing in reflow, and nanostructure formation in memory device fabrication. Moreover, work on crystalline Si (Ref. 2) and Ge (Ref. 3) has strongly suggested that surface vacancies can become charged, leading to changes in the activation energy and preexponential factor for mass transport. This work has further revealed that optical illumination can influence surface diffusion nonthermally by a mechanism that appears to be mediated by changes in vacancy charge state.[4,5] Key applications appear in rapid thermal processing, in which strong lamp illumination is employed.

A particular aspect of surface defect phenomenology that has received significant attention in the literature is the charging of vacancies, both in experimental work by scanning tunneling microscopy[6–10] (STM) and in computational work by density functional theory[11,12] (DFT). Almost all of this work focuses on compound semiconductors, although recent work by Brown *et al.*[10] employed STM to measure charge states of dimer vacancy complexes (pairs and trios) on Si(100)-(2×1). This study revealed that such complexes are positively charged, but determined neither the magnitude of the charge nor the ionization levels.

The present work seeks to expand the understanding of vacancies on Si by using DFT (Ref. 13) to examine isolated divacancies and monovacancies on Si(100)-(2×1). The proximate goal is to determine the identities, structures, and energetics of the stable charge states at 0 K. The identities of the states lend support to the hypothesis outlined above that optically influenced surface diffusion is mediated by changes in vacancy charge state. Artificial tip-induced charging is suggested to have implications for the way STM images are interpreted.

II. COMPUTATIONAL METHOD

The computations employed commercial CASTEP software from Accelrys Inc.[14] Total electronic energies were calculated based on standard DFT methods using the local density approximation. The exchange-correlation term was parametrized following the approach of Perdew and Zunger,[15] an approach whose validity has been well tested in semiconductor systems. The basis functions were plane waves having an energy cutoff of 11 Ry (150 eV). Above this level, variations in calculated formation energies for the various charge states (relative to the neutral) became insignificant. Troullier-Martins pseudopotentials[16] were employed. All calculations were performed at two *k* points {(0, 1/4, 1/4) and (0, −1/4, 1/4)} in the Brillouin zone. Using a finer *k* point mesh did not affect the formation energies significantly.

The surface was modeled as a slab consisting of a 4×4 supercell of the Si(100) unit cell in its well-known 2×1 reconstruction with rows of buckled top-layer dimers. To look for possible symmetry-breaking effects of charging with greater ease, we chose the $p(2\times1)$ rather than the $p(2\times2)$ configuration of the buckled dimers. In the $p(2\times1)$ configuration, the topmost protruding atoms of the dimers are all on the same side of the dimer row, while in the $p(2\times2)$ these topmost atoms alternate to either side of the row when an observer moves from one dimer to the next. The two configurations lie within less than 0.05 eV/dimer of each other,[17] making interconversion between the two facile even at room temperature. The slab consisted of six layers of Si atoms. The space over the surface was treated as a 10-Å-thick vacuum layer, and the dangling Si bonds at the bottom of the slab were saturated with hydrogen atoms.

The monovacancy and divacancy were modeled by respectively removing one and two adjacent Si atoms from a dimer row near the center of the supercell. Note that we left the remaining dimers in the slab in their buckled configuration, so that our procedure departs slightly from quantum calculations performed previously for the divacancy.[18–20] These reports employed the symmetric, unbuckled configuration for the remaining dimers, probably because early the-

oretical work hypothesized that symmetric rows with one-quarter of the dimers replaced by divacancies could be the most stable structure of Si(100)-(2×1).[21] Subsequent quantum calculations sought to confirm or disconfirm this speculation. To our knowledge, there exist no calculations examining the dimer vacancy in conjunction with neighboring buckled dimers, although this configuration almost certainly characterizes real surfaces.

Geometric relaxation of the slab was performed assuming no symmetry constraint, with the top four Si layers allowed to move and the bottom two held fixed in the bulk configuration. Relaxation proceeded in the conventional way until the Hellman-Feynman forces[22] between atoms decreased below 0.1 eV/Å.

Charged systems were modeled by adding to or subtracting from the total number of electrons in a slab and then compensating this charge with a neutralizing jellium background to avoid spurious electrostatic interactions between unit cells.

The calculation described above yields a total energy E_{tot} for a vacancy, but the quantity needed to determine charge state stability is the formation energy. The formation energy E_{vac} of a neutral surface vacancy with respect to the undefected surface can be calculated as[19,23]

$$E_{\mathrm{vac}} = E_{\mathrm{tot},v} + nE_{\mathrm{bulk}} - E_{\mathrm{tot},p}\,, \tag{1}$$

where $E_{\mathrm{tot},v}$ and $E_{\mathrm{tot},p}$ denote the total energies of the defected and perfect surfaces, respectively. E_{bulk} represents the total energy of an atom at a lattice site deep within the bulk, and n denotes the number of atoms that must be removed to create the vacancy. E_{bulk} was calculated separately to be -120.632 eV using a 256-atom bulk slab with periodic boundary conditions on all sides, using the same energy cutoff as for the surface calculations.

The ionization energy required to form a charged defect varies with the position of the Fermi energy E_F because charging requires the transfer of electrons to or from the Fermi level. The total formation energy $E_{\mathrm{vac}}(q)$ for a charged vacancy is the sum of the formation energy of a neutral vacancy [from Eq. (1)] and the ionization energy. If the total formation energy is referenced to that of a neutral vacancy, $E_{\mathrm{vac}}(q)$ obeys the following relation:[12]

$$E_{\mathrm{vac}}(q) = [E_{\mathrm{tot}}(q) - E_{\mathrm{tot}}(0)] + q(E_{\mathrm{VBM}} + E_F), \tag{2}$$

where q denotes the net number of holes supported by the vacancy. The second term in Eq. (2) represents the chemical potential of the electrons in the system. The zero of E_F is taken to be the valence-band maximum. E_{VBM} is normally just the highest occupied energy level for a supercell, but introduction of a defect normally requires a correction to E_{VBM}.[24] The defect can distort the band structure, causing E_{VBM} in a finite supercell to differ considerably from its value in the corresponding infinite supercell. Following the procedure of Matilla and Zunger,[24] we therefore calculated E_{VBM} for our finite defect-containing supercell as follows. The value of E_{VBM} for the undefected supercell was corrected by the difference between two average electrostatic potentials V_{avg}: $V_{\mathrm{avg},d}$ in a bulklike region of the defect-containing supercell and $V_{\mathrm{avg},p}$ in the undefected supercell. The resulting equation for E_{VBM} is

$$E_{\mathrm{VBM}}(\mathrm{defect}) = E_{\mathrm{VBM}}(\mathrm{undefected}) + (V_{\mathrm{avg},d} - V_{\mathrm{avg},p}). \tag{3}$$

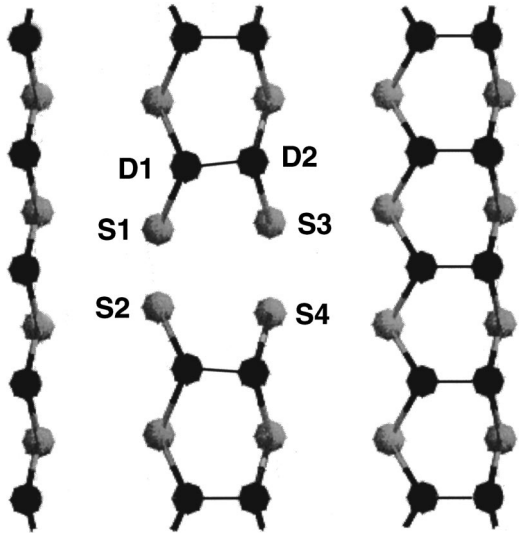

FIG. 1. Top view of the relaxed atomic configuration for a neutral divacancy on Si(100)-(2×1). Gray atoms lie in the second layer, and $S1-S4$ are exposed upon divacancy formation. Black atoms lie in the top (dimer) layer, and $D1$ and $D2$ are a neighboring dimer. $D1$ is the lower atom of this asymmetric dimer and $D2$ the upper. Rebonding causes the $S1$-$S2$ and $S3$-$S4$ pairs to pull closer to each other. The effect is more pronounced for $S1$-$S2$, however, causing the $D1$-$D2$ pair to twist slightly.

III. RESULTS

A. Neutral dimer vacancy

We begin with the neutral divacancy, since it has been studied extensively. Creating a divacancy is tantamount to removing two adjacent atoms in the topmost layer of the dimer row structure. Recall that in the dimer row structure, the rows comprise bilayers of exposed Si atoms. An observer moving along a row sees closely bonded dimers in the topmost layer (labeled D in Fig. 1) alternating with more widely spaced pairs of atoms in an underlying layer (labeled S in Fig. 1). The upper dimer is tilted asymmetrically, creating a corresponding asymmetry in the underlying layer.[17]

Figure 1 shows the atomic configuration that results when a neutral divacancy is formed. As has been shown previously,[18–20] the divacancy induces the adjacent pairs of atoms in the underlying layer ($S1$-$S2$ and $S3$-$S4$) to relax toward and rebond to each other along the row to partially fill the void. Although the $S1$-$S2$ and $S3$-$S4$ distances are identical in the undefected structure, the calculations show that upon divacancy formation the extent of rebonding differs for these pairs of atoms. As shown in Fig. 1 and Table I, the $S1$-$S2$ distance under the lower atom of the original dimer contracts nearly 0.5 Å more than the corresponding $S3$-$S4$ distance under the upper atom. No relaxation asymmetry of this sort appeared in prior work, which employed

TABLE I. Bond lengths of exposed second-layer atoms after divacancy formation.

Charge state	Bond Length (Å)	
	*S*1-*S*2	*S*3-*S*4
Undefected surface	3.84	3.84
0	2.58	3.01
−1	2.62	2.91
−2	2.64	2.97

unbuckled dimers in conjunction with the divacancy. In that work, the distance between the *S*1-*S*2 (or *S*3-*S*4) atoms was calculated at 2.71 Å (Ref. 19) and 2.79 Å (Ref. 20). These distances match closely the *average* of the *S*1-*S*2 and *S*3-*S*4 bond lengths determined here: 2.79 Å.

The agreement with the literature results is notable, since in our calculations only one dimer row separates defects in adjacent cells, while the previously published work employed no such separation. This insensitivity of the results to defect separation across rows can be explained by our observation that electron density corresponding to defects remained localized within the dimer row containing the defect, suggesting that interaction between rows is minimal. The minimal interaction in turn implies that our use of a rather small 4×4 supercell should introduce few errors. The correction applied to the energy of the valence-band maximum (by the method of Matilla and Zunger) should also help to minimize whatever minor errors might be introduced from the proximity of the defects.

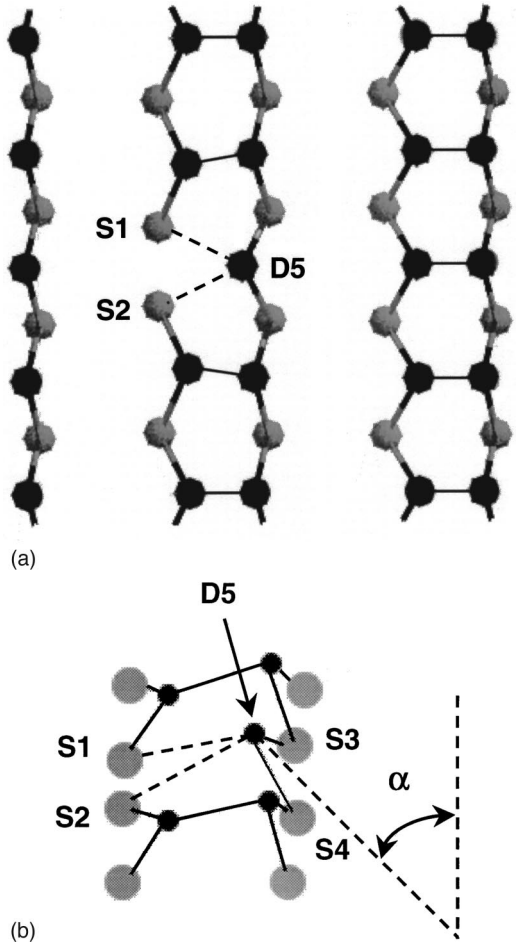

FIG. 2. (a) Top view of the relaxed atomic configuration for a neutral lower monovacancy on Si(100)-(2×1). Atoms *S*1 and *S*2 are the exposed second-layer atoms, which are drawn close to each other by rebonding. *D*5 is the remaining (upper) dimer atom. (b) Side view of the relaxed atomic configuration for the lower monovacancy shown in (a).

TABLE II. Bond lengths of exposed second-layer atoms after monovacancy formation.

Defect type	Charge State	Bond Length (Å)	
		*S*1-*S*2[a]	*S*3-*S*4
Undefected surface		3.84	3.84
Upper	−2	3.73	3.66
	−1	3.73	3.66
	0	3.72	3.66
	+1	3.72	3.66
	+2	4.24	3.62
Lower	0	2.68	3.66
	−1	2.68	3.66

[a]Here *S*1-*S*2 refers to exposed second-layer atoms opposite the remaining dimer atom.

B. Neutral monovacancy

Creating a Si(100)-(2×1) monovacancy is tantamount to removing one atom in the topmost layer (*D* in Fig. 1) of the dimer row structure. Because a dimer pair is tilted asymmetrically, there are two inequivalent ways of creating the monovacancy—by removing either the upper or the lower atom of the pair. The resulting structures are qualitatively similar, but there are quantitative differences in bond lengths, formation energies, and the like.

Figure 2(a) shows the atomic structure in the vicinity of a neutral monovacancy formed by removing the lower dimer atom. This kind of monovacancy induces significant rebonding of the underlying surface atoms. As a quantitative measure of this fact, Table II shows that the distance between the exposed second-layer atoms *S*1 and *S*2 decreases by almost 1.2 Å compared to the undefected surface. Rebonding between these atoms is much less pronounced when the vacancy forms by removal of the upper dimer atom, however. The corresponding distance between exposed second-layer atoms decreases by less than 0.2 Å.

For both kinds of monovacancies, a different kind of rebonding also takes place involving the remaining dimer atom and the exposed second-layer atoms. Figure 2(b) shows this effect for the lower monovacancy. The *S*1 and *S*2 atoms rebond to the remaining dimer atom *D*5, which is drawn even closer to the *S*1 and *S*2 atoms than it is in the undefected structure. In an ideal tetrahedral bonding geometry, the *D*5 atom would stand straight away from the surface, meaning that the plane defined by *D*5 and the underlying *S*3 and

TABLE III. Values for $E_{tot}(q)-E_{tot}(0)$ and E_{VBM} (in eV).

Charge state	Lower monovacancy		Upper monovacancy		Divacancy	
	$E_{tot}(q)-E_{tot}(0)$	E_{VBM}	$E_{tot}(q)-E_{tot}(0)$	E_{VBM}	$E_{tot}(q)-E_{tot}(0)$	E_{VBM}
+2	−0.054	0.242	−0.80	0.333	−0.22	0.401
+1	−0.135	0.124	−0.30	0.286	0	0.243
0	0	0.015	0	0.169	0	0.168
−1	0.725	−0.094	0.68	0.057	0.60	−0.016
−2	1.63	−0.021	1.53	−0.047	1.45	−0.115

$S4$ atoms would be perpendicular to the surface plane. However, this configuration would leave $D5$ with two dangling bonds. So $D5$ tilts over strongly toward $S1$ and $S2$, such that the $D5$-$S3$-$S4$ plane inclines by an angle $\alpha=40°$ away from perpendicular. For comparison, α in the undefected structure is significantly smaller: 18°. A similar, though less pronounced, change in angle occurs when the upper dimer atom is removed; α increases from 60° on the undefected surface to 63.0° upon monovacancy formation. For both kinds of vacancy, rebonding of $D5$ to $S1$ and $S2$ evidently compensates for the strong strain induced by pulling α away from perpendicular. $D5$ interacts equally with $S1$ and $S2$, however; the $D5$-$S1$ and $D5$-$S2$ bond lengths are identical at 3.33 Å for the lower monovacancy and 3.21 Å for the upper.

The relative stabilities of the neutral monovacancy and divacancy can be compared through their formation energies determined by Eq. (1). On a per-atom basis, E_{vac} equals 0.87 eV for the lower monovacancy and 1.50 eV for the upper. The corresponding per-atom formation energy for the divacancy is 0.25 eV, which differs somewhat from the values of 0.11 (Ref. 20) and 0.14 (Ref. 19) eV/atom calculated by previous workers. These latter values, however, were referenced to an undefected surface with unbuckled dimers, while our reference condition incorporates buckled rows. The per-atom formation energy difference between the buckled and unbuckled structures is on the order of 0.1 eV,[17] corresponding closely to the differences between our formation energy and those of Refs. 19 and 20.

The present calculations confirm numerous literature reports that the neutral divacancy is much more stable at 0 K than either neutral monovacancy. The lower monovacancy, however, is much more stable than the upper monovacancy, probably because of the large energy cost associated with the rebonding that forces α up to more than 60°.

C. Charged divacancy

Table III shows the quantities needed to determine formation energies for charged divacancies using Eq. (2) [i.e., $E_{tot}(q)-E_{tot}(0)$ and E_{VBM}]. We performed calculations for charge states ranging from −2 to +2. Equation (1) indicates that the formation energy depends on charge state and the position of the Fermi energy. For a specified Fermi energy, the dominant charge state is the one with the lowest formation energy. Figure 3 plots these energies for the divacancy as a function of E_F. As E_F moves away from the valence band (so that the surface becomes more electron rich), the formation energies of the positive charge states increase (making them more difficult to form), while those of the negative states decrease. The calculations show that divacancies can have stable charge states of −2, −1, and 0, thereby confirming the premise of this paper that multiple charge states can exist on the silicon surface. Positive states are not stable for any value of E_F. For comparison, a divacancy within bulk Si can support charges of −2, −1, 0, and +1.[25,26]

Figure 3 shows that the formation energies of the 0 and −1 states equal each other at $E_F=0.62$ eV. When E_F rests at this so-called "ionization level," the populations of the two charge states are equal to within a spin degeneracy factor of 2 (Ref. 27). The corresponding (−1/−2) level appears at $E_F=1.06$ eV.

These levels lie above the local-density-approximation-(LDA-)calculated band gap of ~0.5 eV, so the possibility existed that the extra electrons put into the calculations merely filled spatially extended states in the conduction band. However, visual inspection of the wave functions showed that the extra electrons remain strongly localized around the defect in both the −1 and −2 cases. Such localization was also observed for all stable charged defects to be discussed below and confirms that true charged defects form in the calculations.

For the surface divacancy, the degree of relaxation of the neighboring atoms does not change significantly with charge state. For example, Table I shows that the bond lengths for

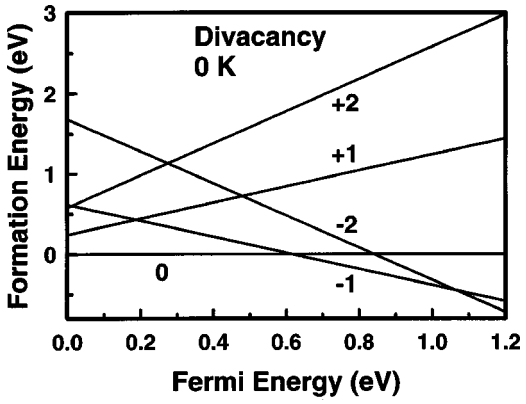

FIG. 3. Formation energies of various charged divacancies on Si(100)-(2×1) as a function of Fermi energy. The formation energy is referenced to the neutral divacancy, while the Fermi energy is referenced to the valence-band maximum.

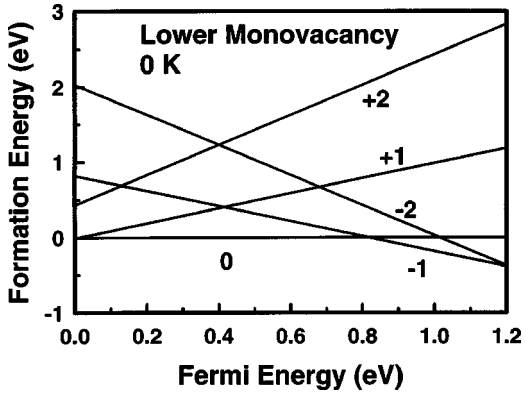

FIG. 4. Formation energies of various charged lower monovacancies on Si(100)-(2×1) as a function of Fermi energy. The formation energy is referenced to the neutral monovacancy, while the Fermi energy is referenced to the valence-band maximum.

rebonded pairs $S1$-$S2$ and $S3$-$S4$ change by less than about 0.1 Å as a result of charging. This change is smaller than comparable changes for the bulk divacancy. *Ab initio* cluster calculations for the bulk divacancy by Ogut and Chelikowsky[28] show charge-induced bond length changes up to 0.2 Å between the −1 and 0 states and up to 0.53 Å for the −2 state.

D. Charged monovacancy

Figures 4 and 5 plot formation energies of charged lower and upper monovacancies, respectively, with the energies referenced to the corresponding neutral species. The lower monovacancy supports only 0 and −1 states, with an ionization level at 0.82 eV. The upper monovacancy, however, supports four stable states: +2, 0, −1, and −2. The corresponding ionization levels are 0.07 eV (+2/0), 0.62 eV (0/−1), and 1.00 eV (−1/−2).

For the lower dimer monovacancy, charging does essentially nothing to alter the surrounding atomic configuration. The negatively charged upper monovacancy exhibits a similar lack of rearrangement. However, the +2 state shows a large increase in the distance between the exposed second-layer atoms $S1$ and $S2$—almost 0.7 Å as shown in Table III. Figure 6(b) shows this stretching pictorially for comparison to the neutral species in Fig. 6(a). The angle α also changes to 66° from 63.0° for the neutral species. This relaxation is apparently responsible for stabilizing the +2 state with respect to the +1.

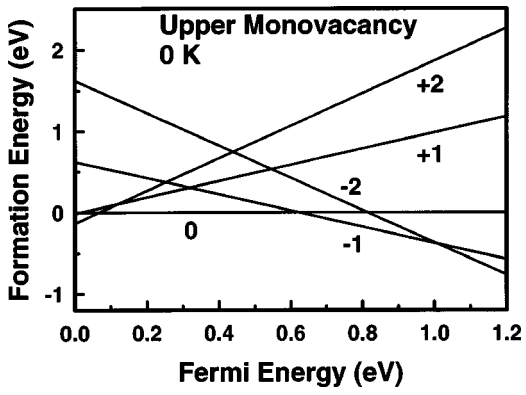

FIG. 5. Formation energies of various charged upper monovacancies on Si(100)-(2×1) as a function of Fermi energy. The formation energy is referenced to the neutral monovacancy, while the Fermi energy is referenced to the valence-band maximum.

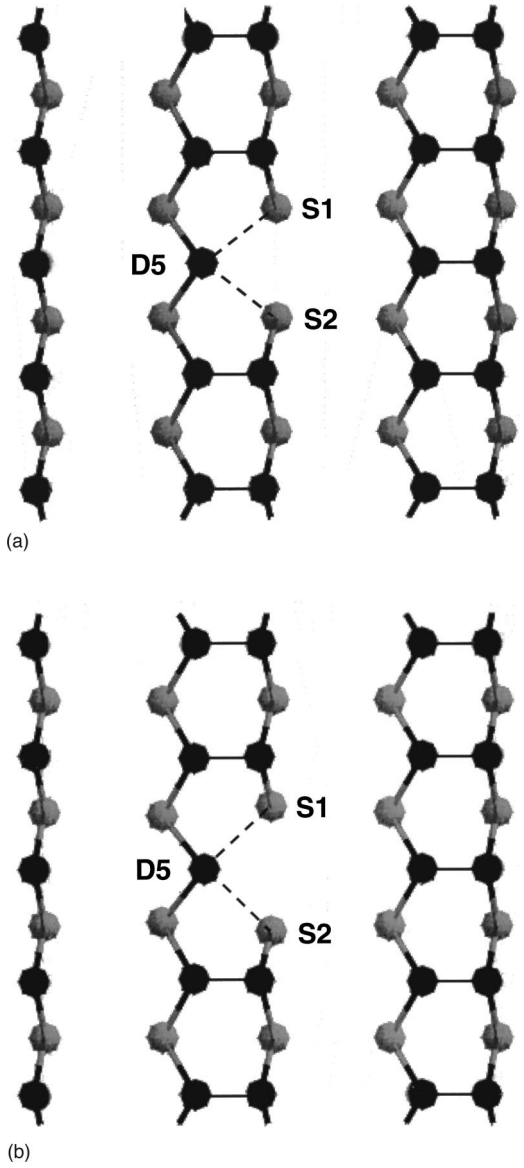

FIG. 6. (a) Relaxed atomic configuration of a neutral upper monovacancy on Si(100)-(2×1). Atoms $S1$ and $S2$ are the exposed second-layer atoms. $D5$ is the remaining dimer atom. (b) Relaxed atomic configuration of a +2 upper monovacancy on Si(100)-(2×1). Atoms $S1$ and $S2$ are the exposed second-layer atoms. $D5$ is the remaining dimer atom

In fact, the absence of the +1 state corresponds to so-called ''negative-U'' behavior, in which the removal of one electron from the neutral defect leads immediately to the removal of a second. Such behavior is common for vacancy[29] and interstitial[30] defects in bulk Si, notably for the +1 state of the bulk monovacancy,[29] which has been studied extensively for nearly three decades. The bulk monovacancy exhibits significant Jahn-Teller distortion of the nearest-

neighbor atoms for all charge states.[31,32] Several kinds of relaxations exist whose natures are still debated,[33] but they are large enough that ionization from the neutral to the $+2$ state proceeds without stopping at the $+1$.[34,35] Our results give evidence for analogous behavior on Si(100), which to our knowledge has not been observed before for a semiconductor surface.

IV. DISCUSSION

A. Dominant charge states at 0 K

It is clear that vacancies on Si(100) can support different charge states depending on the position of the surface Fermi level. There is a sizable body of literature that has attempted to discern this position. Himpsel *et al.*[36] reported that E_F on undoped Si(100)-(2×1) lies 0.34 eV above the valence-band maximum based on core-level photoelectron emission at room temperature. However, in their calculation they based this result on an early value for $E_F - E_{\mathrm{VBM}} = 0.33$ eV reported for cleaved Si(111)-(2×1) by Allen and Gobeli.[37] Himpsel *et al.*[38] subsequently made improved photoemission measurements on this material to yield a value of 0.40 eV. Thus the value reported for Si(100)-(2×1) must be readjusted to 0.41 eV.

There is in principle a dependence of this number on both doping level and temperature. Regarding doping level, the data of Himpsel *et al.* for Si(111)-(2×1) show that $E_F - E_{\mathrm{VBM}}$ increases by about 0.2 eV for strong *n* doping and decreases by the about the same amount for strong *p* doping. For Si(100)-(2×1), a surface photovoltage study by Mönch *et al.*[39] reports a spread in $E_F - E_{\mathrm{VBM}}$ of 0.30 eV between *n*-type and *p*-type material at 85 K. Although these workers did not examine undoped material, it seems reasonable based on the behavior for Si(111)-(2×1) to estimate $E_F - E_{\mathrm{VBM}}$ for undoped Si(100)-(2×1) using the average of their results for *n*- and *p*-type Si. This average is 0.43 eV—close to the value of 0.41 eV calculated above. Regarding the temperature dependence, Mönch *et al.*[39] also showed that E_F moves less than 0.1 eV from room temperature to 85 K. Similarly, the invariance of features within photoemission spectra reported by Cricenti *et al.* on Si(100)-(2×1) suggests that E_F remains constant to within 0.1 eV up to 1200 K.[40] Taken together, these results imply the position of E_F remains constant to within about 0.1 eV down to 0 K where the present calculations were performed.

With $E_F - E_{\mathrm{VBM}}$ at 0.41 eV, Figs. 3–5 imply that both divacancies and monovacancies are predominantly in the neutral state at low temperatures.

B. Charge state identities: Implications for surface diffusion

There is significant evidence that nonthermal effects of optical illumination on surface diffusion are mediated by charged surface vacancies whose population statistics vary in response to the generation of photogenerated charge carriers. As discussed elsewhere,[4,5] the evidence comes from several observations. First, the magnitudes of the observed *changes* in activation energy and preexponential factor remain invariant for three different adsorbates on Si(111), pointing to a single common mediating entity. Second, the effects do not depend on the illumination wavelength as long as the photon energy exceeds the substrate band gap, implicating carrier photogeneration as a key factor. Third, the magnitude of the illumination-induced change increases logarithmically with intensity with a magnitude comparable to that for motion of the quasi-Fermi level for minority carriers. One would expect such behavior if vacancy concentrations depended on the relative positions of this quasi-Fermi level and an ionization level.

This line of reasoning relies at least tacitly on the ability of surface vacancies to support more than one charge state. Measurements of purely thermal surface diffusion have offered evidence for this hypothesis,[2] and analogies with vacancy charging effects in the bulk give additional support. However, proof was lacking. The present calculations offer much stronger evidence that vacancies on Si surfaces can exist in different charge states whose relative populations depend on the position of the surface Fermi level. Since the results pertain to Si(100) at 0 K, whereas the observations were made on Si(111) at high temperature, a more direct connection can unfortunately not be made between the computations and experiments.

C. Implications for artifacts in STM imaging

It is known that STM sometimes induces changes in surface structure. For example, tip-induced surface charge can alter the most favorable reconstruction of W(100).[41] However, the existing literature on STM imaging of vacancies on semiconductors does not discuss the possibility of changes in charge state induced by tunneling current from the tip. Such changes are quite possible if charge injected into the vacancy by the tip does not leak away quickly into the surrounding substrate material. The tight spatial charge localization near vacancies shown by our calculations, coupled with the positions of the ionization levels deep within the band gap, make slow charge leakage at least plausible.

The effects of such artificial charging on the resulting image would depend on the extent to which the surface Fermi energy is pinned. Lack of pinning [on cleaved GaAs(110) (Ref. 9) or Si(100)-(2×1) with few "*C*"-type defects (Ref. 10), for example] permits charge localized near a vacancy to produce a large and characteristic local signature in STM images. This signature tends to obscure the geometrical structure of the underlying vacancy.[9] Thus, although it may be difficult to determine whether such a signature (or lack thereof, if tip actually neutralizes a charged defect) is an artifact induced by tunneling from the tip, there is little chance that the image will offer structural information about the defect as it actually appears in the image.

In the presence of Fermi-level pinning, however, the characteristic signature of charging no longer appears to obscure the underlying structure, and the vacancy's geometry can be probed. If image analysis is performed without recognition that artificial tip-induced charging may be taking place, then charge-induced structural rearrangements of the sort described in previous sections might be interpreted as the actual thermodynamically stable geometry. In the case of the

upper monovacancy, for example (hypothetical, because it is not very stable), tunneling at a surface bias sufficiently positive to convert the neutral state to +2 would make the $S1$-$S2$ bond length appear 0.7 Å longer than it actually is.

V. CONCLUSIONS

First-principles calculations based on density functional theory have been performed to investigate the charging of divacancies and monovacancies on Si(100)-(2×1). The results have offered strong evidence for the existence of multiple charge states whose individual stabilities depend on the position of the surface Fermi level. The behavior roughly mimics that of analogous defects in the bulk, including the appearance of negative-U behavior. It is plausible to believe that the existence of such states and the structural rearrangements that accompany them generalize to many kinds of semiconductors, with implications for surface diffusion and STM imaging.

ACKNOWLEDGMENTS

This work was partially supported by the NSF Grant No. (CTS 98-06329). H.Y.C. acknowledges support of the DOE (Grant No. DEFG02-91ER45439) through the Materials Research Laboratory at UIUC and through the Department of Chemical Engineering. Computations were performed with support from the National Computational Supercomputing Alliance at UIUC.

*Author to whom correspondence should be addressed. Electronic address: eseebaue@uiuc.edu

[1] E. G. Seebauer and C. E. Allen, Prog. Surf. Sci. **49**, 265 (1995); E. G. Seebauer and M. Y. L. Jung, in *Numerical Data and Functional Relationships: Adsorbed Layers on Surfaces*, Landolt-Börnstein, New Series, Group III, Vol. III/42A, edited by H. P. Bonzel (Springer-Verlag, New York, 2001), Chap. 11.
[2] C. E. Allen, R. Ditchfield, and E. G. Seebauer, J. Vac. Sci. Technol. A **14**, 22 (1996).
[3] I. I. Suni and E. G. Seebauer, J. Chem. Phys. **100**, 6772 (1994).
[4] R. Ditchfield, D. Llera-Rodriguez, and E. G. Seebauer, Phys. Rev. Lett. **81**, 1259 (1998).
[5] R. Ditchfield, D. Llera-Rodriguez, and E. G. Seebauer, Phys. Rev. B **61**, 13 710 (2000).
[6] Ph. Ebert, X. Chen, M. Heinrich, M. Simon, K. Urban, and M. G. Lagally, Phys. Rev. Lett. **76**, 2089 (1996).
[7] Ph. Ebert, K. Urban, and M. G. Lagally, Phys. Rev. Lett. **72**, 840 (1994).
[8] G. Lengel, R. Wilkins, G. Brown, M. Weimer, J. Gryko, and R. E. Allen, Phys. Rev. Lett. **72**, 836 (1994).
[9] Ph. Ebert, Surf. Sci. Rep. **33**, 121 (1999).
[10] G. W. Brown, H. Grube, M. E. Hawley, S. R. Schofield, N. J. Cursons, M. Y. Simmons, and R. G. Clark, J. Appl. Phys. **92**, 820 (2002).
[11] H. Kim and J. R. Chelikowsky, Phys. Rev. Lett. **77**, 1063 (1996).
[12] S. B. Zhang and A. Zunger, Phys. Rev. Lett. **77**, 119 (1996).
[13] M. C. Payne, M. P. Teter, D. C. Allan, T. A. Arias, and J. D. Joannopoulos, Rev. Mod. Phys. **64**, 1045 (1992).
[14] V. Milman, B. Winkler, J. A. White, C. J. Pickard, M. C. Payne, E. V. Akhmatskaya, and R. H. Nobes, Int. J. Quantum Chem. **77**, 895 (2000).
[15] J. Perdew and A. Zunger, Phys. Rev. B **23**, 5048 (1981).
[16] N. Troullier and J. L. Martins, Phys. Rev. B **43**, 1993 (1991).
[17] A. Ramstad, G. Brocks, and P. J. Kelly, Phys. Rev. B **51**, 14 504 (1995).
[18] J. H. G. Owen, D. R. Bowler, C. M. Coringe, K. Miki, and G. A. D. Briggs, Surf. Sci. **341**, L1042 (1995).
[19] N. Roberts and R. J. Needs, Surf. Sci. **236**, 112 (1990).
[20] J. Wang, T. A. Arias, and J. D. Joannopoulos, Phys. Rev. B **47**, 10 497 (1993).
[21] K. C. Pandey, in *Proceedings of the 17th International Conference on the Physics of Semiconductors*, edited by D. J. Chadi and W. A. Harrison (Springer, New York, 1985), p. 55.
[22] R. P. Feynman, Phys. Rev. **56**, 340 (1939).
[23] H. Lim, K. Cho, R. B. Capaz, and J. D. Joannopoulos, Phys. Rev. B **53**, 15 421 (1996).
[24] T. Matilla and A. Zunger, Phys. Rev. B **58**, 1367 (1998).
[25] A. O. Evwaraye and E. Sun, J. Appl. Phys. **47**, 3776 (1976).
[26] L. C. Kimerling, P. Blood, and W. M. Gibson, in *Proceedings of the International Conference on Radiation Effects in Semiconductors, Nice, 1978*, edited by J. H. Albany (IOP, London, 1979).
[27] The −1 and +1 states each have an unpaired electron with possible up- and down-spin states. The −2, 0, and +2 states have no such degeneracy. Thus at the 0/+1 ionization level, for example, $[V^+]=2[V^0]$. See J. A. Van Vechten, Phys. Rev. B **33**, 2674 (1986).
[28] S. Ogut and J. R. Chelikowsky, Phys. Rev. Lett. **83**, 3852 (1999).
[29] M. J. Puska, S. Pöykkö, M. Pesola, and R. M. Nieminen, Phys. Rev. B **58**, 1318 (1998).
[30] R. D. Harris, J. L. Newton, and G. D. Watkins, Phys. Rev. Lett. **48**, 1271 (1982).
[31] O. Sugino and A. Oshiyama, Phys. Rev. Lett. **68**, 1858 (1992).
[32] S. Ogut, H. Kim, and J. R. Chelikowsky, Phys. Rev. B **56**, 11 353 (1997).
[33] A. Antonelli, E. Kaxiras, and D. J. Chadi, Phys. Rev. Lett. **81**, 2088 (1998).
[34] G. A. Baraff, E. O. Kane, and M. Schluter, Phys. Rev. B **21**, 5662 (1980).
[35] G. D. Watkins and J. R. Troxell, Phys. Rev. Lett. **44**, 593 (1980).
[36] F. J. Himpsel, P. Heimann, T.-C. Chiang, and D. E. Eastman, Phys. Rev. Lett. **45**, 1112 (1980).
[37] F. G. Allen and G. W. Gobeli, Phys. Rev. **127**, 150 (1962).
[38] F. J. Himpsel, G. Hollinger, and R. A. Pollak, Phys. Rev. B **28**, 7014 (1983).
[39] W. Mönch, P. Koke, and S. Krueger, J. Vac. Sci. Technol. **19**, 313 (1981).
[40] A. Cricenti, D. Purdie, and B. Reihl, Surf. Sci. **331–333**, 1033 (1995).
[41] J. G. Che, Z. Z. Zhu, and C. T. Chan, Phys. Rev. Lett. **82**, 3292 (1999).